Experimental Assessment of the Time Transfer Capability of Precise Point Positioning (PPP)

Diego Orgiazzi, Patrizia Tavella
Time and Frequency Metrology Department
Istituto Elettrotecnico Nazionale "Galileo Ferraris" (IEN)
Torino, Italy
orgiazzi@ien.it

François Lahaye
Geodetic Survey Division
Natural Resources Canada (NRCan)
Ottawa, Canada
Francois.Lahaye@nrcan.gc.ca

***Abstract*—In recent years, many national timing laboratories have installed geodetic Global Positioning System (GPS) receivers together with their traditional GPS/GLONASS Common View (CV) receivers and Two Way Satellite Time and Frequency Transfer (TWSTFT) equipment. A method called Precise Point Positioning (PPP) is in use in the geodetic community allowing precise recovery of geodetic GPS receiver position, clock phase and tropospheric delay by taking advantage of the International GNSS Service (IGS) precise products. Natural Resources Canada (NRCan) has developed software implementing the PPP and a previous assessment of the PPP as a promising time transfer method was carried out at Istituto Elettrotecnico Nazionale (IEN) in 2003. This paper reports on a more systematic work performed at IEN and NRCan to further characterize the PPP method for time transfer application, involving data from nine national timing laboratories. Dual-frequency GPS observations (pseudorange and carrier phase) over the last ninety days of year 2004 were processed using the NRCan PPP software to recover receiver clock estimates at five minute intervals, using the IGS Final satellite orbit and clock products. The quality of these solutions is evaluated mainly in terms of short-term noise. In addition, the time and frequency transfer capability of the PPP method were assessed with respect to independent techniques, such as TWSTFT, over a number of European and Transatlantic baselines.**

I. INTRODUCTION

Time and frequency transfer using GPS code and carrier-phase is a research activity for many institutions involved in time applications [1],[2]. This was certainly recognized when the IGS (International GNSS Service) and BIPM (Bureau International des Poids et Mesures) formed a joint pilot study [3] to analyze the IGS Analysis Centers (ACs) clock solutions and recommend new means of combining them. That study resulted in the formation of the Final and Rapid IGS time scales [4] as respective time reference for the Final and Rapid IGS combined clock products (both station and satellites) produced since fall 2000 [5].

Whereas all IGS ACs clock solutions are network-based, software and methods are available to use network-based products to process single stations receiver data, mainly as a cost-effective way to "densify" solutions, be it earth stations positions, clocks or local tropospheric parameters. This paper reports on follow-on work jointly performed at Istituto Elettrotecnico Nazionale (IEN) "Galileo Ferraris", Turin, Italy, and at Natural Resources Canada (NRCan), Ottawa, Canada, to assess the time transfer potential of such a method, named Precise Point Positioning (PPP) [6]. PPP is a geodetic single station post-processing method for recovering coordinates of GPS reception antennas, GPS receiver clock offsets and local tropospheric parameters. It has been shown that PPP clock solutions are consistent with IGS Final clock products at the sub-nanosecond level [7],[8]. PPP solutions are also consistent at the 2 ns level with other relative measurement techniques, i.e. Two Way Satellite Time and Frequency Transfer (TWSTFT), GPS Common View (CV) and GPS P3 [9]. Finally, PPP shows a 2-time improvement in stability over GPS CV and GPS P3, providing a frequency stability (in terms of Allan deviation) of $1 \cdot 10^{-14}$ at one day [7].

The objectives of the present work are:

- to confirm the preliminary results by analyzing longer datasets from multiple national timing laboratories;
- to further assess the PPP frequency stability at short-term (less that one day) and long-term (more than one day);
- to address the issues raised in [7], specifically the clock series discontinuities caused either artificially by the 1-day batch processing or by real receiver loss-of-lock on satellites signals.

The remainder of this section provides background information on NRCan's implementation of the PPP algorithm. Then, the datasets collected for the analysis are described. Timing-specific improvements implemented to

0-7803-9052-0/05/$20.00 © 2005 IEEE.

NRCan PPP for this experiment are presented and discussed, as well as the quality of the geodetic solutions. Finally, the PPP station clock time series are analyzed with respect to both the IGS Final clock products and the TWSTFT over a number of selected European and Transatlantic baselines.

II. PRECISE POINT POSITIONING

A. NRCan's Algorithm

NRCan's implementation of the PPP method was originally developed as a geodetic tool to provide station-positioning capability within geodetic reference frames. The PPP method is a post-processing approach using un-differenced observations coming from a single geodetic GPS receiver along with satellite orbits and clocks, and modeled ionospheric delays for single frequency receivers.

The parameters estimated in PPP are station positions (in static or kinematic mode), station clock states, local troposphere zenith delays and carrier phase ambiguities. The best position solution accuracies, reaching the few centimeters in horizontal coordinates and less than 10 cm in vertical coordinates (RMS), are obtained by processing dual-frequency pseudorange and carrier phase observations together with high-quality GPS orbit and clock products, such as those provided by the IGS.

NRCan PPP can achieve this using accurate models for all the physical phenomena involved. Further details on the PPP algorithms, models and specifications can be found in [6].

B. Timing Specific Improvements

For purpose of the experiment reported in this paper, the NRCan PPP software was updated to address the intra-solution and solution-boundary station clock discontinuities.

Concerning the artificial solution-boundary discontinuities, the software was changed to allow processing of RINEX-format [10] observation files that span multiple-days (currently up to a maximum of 14). In this multiple-day processing, precise satellite orbit and satellite clock information from IGS are input as daily files. Major findings about the multi-day processing are discussed in section IV.C.

However, since concatenating RINEX data files is operationally cumbersome and certainly awkward considering the current *de-facto* IGS standard of daily files, this change is viewed as a preliminary proof of concept only. Future upgrades to the NRCan PPP software will allow continuous processing of consecutive daily RINEX-format observation files.

Concerning intra-solution discontinuities, an attempt was made to use the *a-priori* knowledge of the clock state and to propagate its value taking into account the noise characteristics of the reference frequency standards (i.e., atomic clocks as Cesium or hydrogen maser) to help in the estimation process of newly introduced ambiguities. Specifically, the user can set a station clock process noise value that will be used as *a-priori* weight for the *a-priori* epoch clock value, computed from an internal station clock model. At this time, this internal model is a one-state model, i.e. essentially the last estimate of the station clock, which is suitable only for steered frequency standards affected by white frequency noise. Also, the clock model does not accommodate real receiver clock resets, i.e. events when the station clock offset process noise should be relaxed. Preliminary results concerning clock process noise constraints are reported in section IV.B.

III. EXPERIMENT SET-UP

A. Selected Timing Laboratories

For the purpose of this experiment, nine worldwide

TABLE I. GEODETIC STATIONS AND ASSOCIATED EQUIPMENT FOR SELECTED TIMING LABORATORIES

Laboratory (TAI acronym)	Country	IGS Station	Receiver	External Frequency	Time Links
USNO	USA	USN3	ASHTECH Z-12T	H-maser	TWSTFT, GPS P3
NIST	USA	NISU	NOVATEL	H-maser	TWSTFT
PTB	Germany	PTBB	ASHTECH Z-12T	Laboratory Cesium	TWSTFT, GPS P3
NPL	UK	NPLD	ASHTECH Z-12T	H-maser	TWSTFT, GPS P3
OP	France	OPMT	ASHTECH Z-12T	H-maser	TWSTFT, GPS P3
IEN	Italy	IENG	ASHTECH Z-12T	Industrial Cesium	TWSTFT, GPS P3
NICT	Japan	KGN0	ASHTECH Z-12T	Industrial Cesium	TWSTFT, GPS P3
NRC	Canada	NRC3 [a]	ASHTECH Z-12T	H-maser	GPS P3
ORB	Belgium	BRUS	ASHTECH Z-12T	H-maser	GPS P3

a. "NRC3" is actually collocated at the National Research Council of Canada (NRC) facilities with the "NRC1" IGS station.

national timing laboratories were involved (Table I). They were selected among the timing laboratories which

- regularly contribute to the BIPM realization of the International Atomic Time (TAI),
- operate at least one TWSTFT station, regularly performing measurement sessions with other laboratories, and
- operate a dual-frequency geodetic GPS receiver, which is preferably part of the IGS network allowing then for direct comparison with IGS clock products.

A preliminary assessment of local code multipath levels was also performed over a period of 20 days, from October 26th, 2004 to November 15th, 2004, to verify the tracking quality of the selected timing laboratories' geodetic receivers.

B. GPS Data

A dataset of dual-frequency GPS pseudorange and carrier phase observations, collected during the period from October 3rd, 2004 (MJD 53281) to January 1st, 2005 (MJD 53371), was assembled from the daily RINEX files at 30 seconds sampling available from the IGS data centers. This 91-day period fully overlaps the 20-day comparison campaign of Cesium (Cs) fountain Primary Frequency Standards (PFS) [11], where multiple synchronization techniques were analyzed in detail for 5 of the 9 selected timing laboratories (NIST, PTB, NPL, OP, and IEN).

After an initial processing of the data, some station-days were rejected due to tracking problems that NRCan PPP could not process correctly due to various types of code-phase inconsistencies (see, e.g. [12]).

C. TWSTFT Data

Looking at Table I, seven of the nine worldwide timing laboratories (USNO, NIST, PTB, NPL, OP, IEN, and NICT) provide access to the TWSTFT technique. These laboratories perform TWSTFT measurements following the standard procedures issued by the CCTF Working Group on TWSTFT [13]. In particular, a nominal schedule with 4 measurement sessions per day (at 0h, 8h, 14h and 16h UTC) is regularly followed since January 2004. Each 2-minute session at each pair of stations consists of 120 measurements (1 per second), which are then processed following ITU-R Recommendations [14].

For the purpose of this experiment, only an intensified schedule with up to 12 sessions per day (nominally once every 2 hours), performed by laboratories involved in Cs PFS comparison [11], was considered.

D. PPP Processing Options

The two timing specific improvements cited in section II.B were included in Release 1365 of version 1.04 NRCan PPP, which was used for the present analysis.

All stations datasets were processed in 1-day, 1-week, and 2-week continuous solutions, without applying constraints to the station clock process noise (hereafter called "open" solutions). Moreover, the 1-week and 2-week continuous solutions were also performed with constraints on the station clock process noise (hereafter called "constrained" solutions), which means considering the previous clock state estimate as initial value for the new batch affected by the specified level of white frequency noise. The process noise values were derived from a stability assessment of the 1-day "open" clock time series (Table II). OPMT station was excluded from these "constrained" solutions, because the PPP internal one-state clock model could not handle its free-running H-maser. Also, NISU and USN3 stations were excluded due the number of receiver clock resets, as well as a few station-days that also exhibited receiver clock resets.

TABLE II. STATION CLOCK PROCESS NOISE

Station	Allan Deviation @ 300 s (units of 10^{-14})	Resulting Process Noise Variance (10^{-3} ns^2)
BRUS	4.4	0.17
IENG	53.8	26.00
KGN0	37.2	12.40
NPLD	4.4	0.17
NRC3	4.1	0.15
PTBB	34.2	10.50

All PPP processing were performed using IGS Final 15-minute satellite orbit and 5-minute satellite clock products. The station position was estimated in static mode (i.e., one constant position per continuous processing period) with epoch station clock and local tropospheric zenith delay at 5-minute intervals, synchronized with the satellite precise clock epochs. The tropospheric zenith delays were estimated as a process noise of 5 cm/hour$^{1/2}$.

To be consistent with the IGS clock products that are generated based on a P1 and P2 ionosphere-free combination, all stations were processed using P1 and P2 pseudoranges, except for station NISU that observed only C/A and P2. In that case, the C/A observations were corrected for the C1-P1 biases published by the IGS [15].

IV. PROCESSING RESULTS

A. Geodetic Solutions

All 1-day, 1-week, and 2-week PPP position solutions of IGS stations were compared to the IGS Final weekly combination. For the NRC3 and NISU stations, which were not included in IGS solutions at the time of experiment, PPP position solutions were compared with an average value over all PPP solutions.

Table III shows the RMS of differences in horizontal components (H-RMS $=\sqrt{RMS(lat)^2 + RMS(lon)^2}$) and vertical component (V-RMS). It can be seen that the solutions are in agreement with the IGS (or the mean) at better than 1 cm in horizontal components and better than 2 cm in vertical. This is consistent with typical PPP positioning quality [6].

Moreover, as far as the position solution is concerned, the clock "constrained" solutions provided the same quality as the "open" solutions and processing longer datasets slightly reduced the variability of position solutions.

TABLE III. PPP POSITIONING SOLUTIONS VERSUS IGS COMBINATION

	Station	Open (cm)			Constrained (cm)
		1-day	*1-week*	*2-week*	*1-week*
H-RMS	BRUS	0.6	0.5	0.4	0.5
	IENG	0.8	0.4	0.4	0.4
	KGN0	0.6	0.4	0.2	0.4
	NISU	0.8	0.7	0.6	
	NPLD	0.8	0.5	0.4	0.5
	NRC3	0.5	0.6	0.6	0.6
	OPMT	0.7	0.5	0.4	
	PTBB	0.7	0.3	0.3	0.3
	USN3	0.8	0.5	0.5	
V-RMS	BRUS	0.7	0.4	0.3	0.4
	IENG	1.9	0.7	0.4	0.7
	KGN0	1.3	1.7	1.4	1.7
	NISU	1.0	0.5	0.4	
	NPLD	0.7	0.4	0.3	0.4
	NRC3	1.2	0.5	0.4	0.4
	OPMT	1.0	0.4	0.3	
	PTBB	1.4	0.4	0.3	0.4
	USN3	1.0	0.7	0.6	

B. *Station Clock Process Noise Constraint*

Whereas the objective of constraining the station clock process noise is to reduce the impact of real phase discontinuities on the clock solution, it must not artificially improve its quality by enforcing too tight a constraint. It was already mentioned that the constraints applied did not affect the position solution with respect to the "open" solution (section IV.A).

Differencing "constrained" and "open" 1-week clock solutions, it is apparent that for most stations the clock constraint did not significantly affect the solutions, particularly for Cs frequency standard stations (i.e., IENG, KGN0, and PTBB) whereas H-maser equipped stations (i.e., BRUS, NPLD, and NRC3) seem slightly over-constrained.

Over all the processed station-days, there were only 3 clear-cut cases of ambiguity resets due to loss of lock, summarized in Table IV. Here, the clock discontinuities introduced by loss of lock were significantly reduced when the constraint was applied, as also clearly depicted in Fig. 1 for the NRC3 station.

All other ambiguity resets resulted from significant gaps in the tracking data (over which it is unreasonable to apply any constraint on the station clock parameter), or cases of code-phase inconsistencies or receiver clock resets.

TABLE IV. AMBIGUITY RESETS DUE TO LOSS OF LOCK

Station	Epoch		Discontinuity (ps)	
	DOY (2004)	*GPS Time*	*Open*	*Constrained*
KGN0	315	12:35:00	-111	-9
NRC3	312	23:55:00	-389	-1
	313	01:00:00	399	2

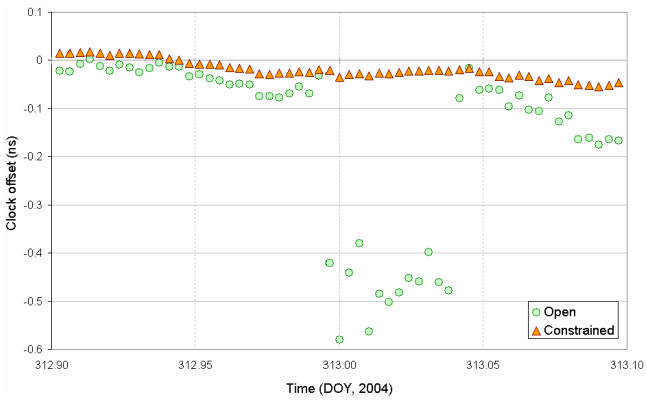

Figure 1. PPP estimate of NRC3 station clock offset (1-week PPP solution), with two ambiguity resets affecting "open" solution.

These preliminary results of the clock constraint are encouraging. Further work is needed to implement internal clock models that accommodate a larger class of frequency standards as well as real receiver clock resets. Tuning of the input constraint value also needs better defining principles, especially for H-maser stations.

C. *Multi-day Continuous Processing*

In order to evaluate clock discontinuities at certain epochs (i.e., day-boundary, week-boundary, etc), all station clock series provided by PPP were fitted to a linear model over 15-day intervals, with intervals overlapping each other by 1 day. The clock series differences with respect to their model and the change in these clock differences between 5-minute epochs over specific boundaries were then computed, leading to estimates of boundary discontinuities.

Table V reports the average absolute value of these boundary discontinuities for "open" solutions over 1 day, 1 week and 2 weeks, respectively. Day-boundary clock discontinuities, that were effectively solution-boundary in 1-day solutions, are considerably reduced in 1-week and 2-week solutions, more so for H-maser than for the Cs equipped stations, but significantly for both. However, residual day-boundary discontinuities can still be noticed in both 1-week and 2-week solutions, at the level of less than 100 ps for H-maser equipped stations.

In contrast, solution-boundary clock discontinuities for the 1-week and 2-week solutions show a slight increase with increasing length of processing interval. Although not very conclusive due to the small number of 1-week (12) and 2-week (6) solution-boundary data, this fact seems to be due to some un-modeled signals in the GPS observables, but this matter is currently under investigation at NRCan.

TABLE V. SOLUTION-BOUNDARY STATISTICS PER STATION

Station	Day-boundary (ps)			Week-boundary (ps)	Biweek-boundary (ps)
	1-day	*1-week*	*2-week*		
BRUS	116	67	66	123	108
IENG	175	142	140	180	210
KGN0	177	139	133	166	149
NPLD	191	82	71	261	244
NRC3	99	78	77	144	165
PTBB	150	102	105	119	143
USN3	226	86	89	187	293

Since all clock datum issues affect station clocks, ambiguities and pseudoranges, the effect of reducing day-boundary clock discontinuities on the PPP pseudorange residuals were analyzed.

The pseudorange residuals, i.e. observed pseudoranges minus modeled ranges, were averaged over 1-day intervals. These daily averages of pseudorange residuals were then differenced between adjacent days, leading to an estimate of the datum change on the pseudorange between days. Table VI shows the average absolute value of the changes in daily pseudorange residuals average for the different solution intervals and for each station.

It follows that such residuals significantly increase in multi-day continuous processing (especially from 1-day to 1-week solutions), which would be consistent with the hypothesis that solution-boundary discontinuities are a result of averaging properties of the code observations PPP residuals.

TABLE VI. DAILY PSEUDORANGE RESIDUALS PER PPP SOLUTIONS

Station	Average absolute value (ps)		
	1-day	*1-week*	*2-week*
BRUS	45	107	106
IENG	32	140	135
KGN0	35	96	99
NISU	40	451	466
NPLD	25	187	181
NRC3	21	93	85
OPMT	65	273	300
PTBB	46	115	118
USN3	38	221	222

V. COMPARISON WITH IGS CLOCK PRODUCTS

Concerning the agreement versus IGS Final clock products (available as daily files only), the residuals between clock estimates show evidence of a very small RMS, namely less than 130 ps for all individual stations and even better in some cases (i.e., NPLD and OPMT, both equipped with H-maser), as summarized in Table VII.

TABLE VII. RESIDUALS BETWEEN PPP AND IGS FINAL CLOCK PRODUCTS

Station	Average (ps)	RMS (ps)
BRUS	-75	118
IENG	74	111
KGN0	76	126
NPLD	8	72
OPMT	40	76
PTBB	-25	126
USN3	-42	111
Average	8	106

In term of frequency stability, the Allan deviation plotted in Fig. 2 for baseline between BRUS and NPLD shows that PPP 1-day solution performs as well as IGS Final clock products for all averaging times. This means that no additional measurement noise is introduced by the single-station estimation method performed by PPP.

Moreover, Fig. 2 shows a clear improvement with longer period of continuous processing (2 weeks in this case). Nevertheless, it is worth mentioning that both PPP solutions differ from IGS clock products with a significant "bump" for observation times close to $2 \cdot 10^4$ seconds. This matter is currently under investigation at NRCan and it could be due to a mismodelled parameter in the PPP algorithm.

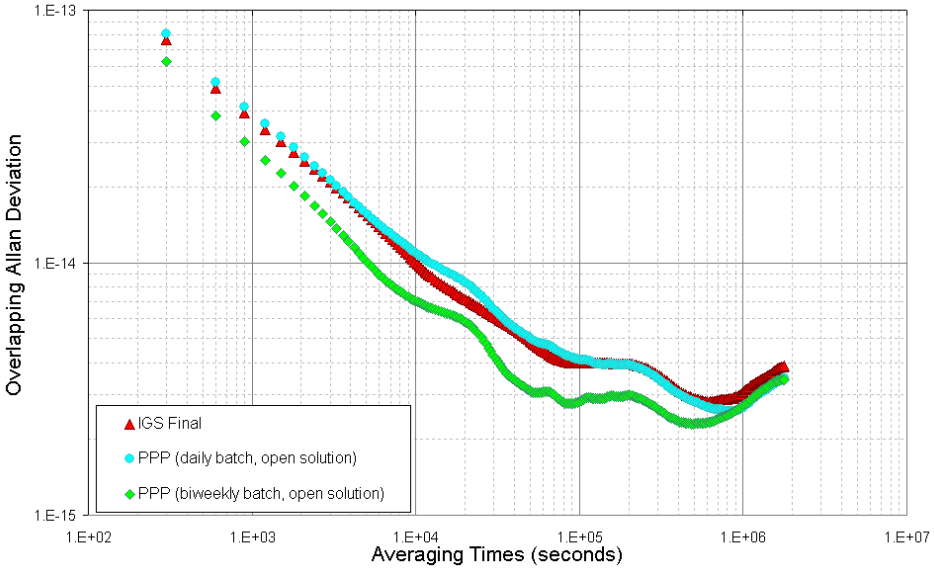

Figure 2. Frequency stability comparison (in term of Allan deviation) between PPP 1-day solution (blue circles), PPP 2-week solution (green diamonds) and IGS Final clock products (red triangles) for the BRUS-NPLD link between ORB and NPL timing laboratories.

VI. COMPARISON WITH TWSTFT

In this experiment the capabilities of the PPP method, in terms of time and frequency transfer, were evaluated versus TWSTFT data for the three baselines in Table VIII, involving three timing laboratories equipped with H-maser. Of course, a more complete comparison between the two methods involving an extended set of baselines and longer period is an important concern for future work. These results are to be considered as preliminary.

Aiming to avoid injection of any artificial effects by the addition of new PPP timing features, 2-week PPP solutions without constraints on the clock process noise have been considered here. Also, only the TWSTFT intensive measurement schedule campaign (12 sessions per day, 2 hours equally spaced) is used, in order to get a larger set of comparison data.

TABLE VIII. BASELINES FOR PPP TO TWSTFT COMPARISON

Baseline	Type	Length	Interval (DOY, 2004)
OP – NPL	European	345 km	299.5 ÷ 326.2
OP – NIST	Transatlantic	7 388 km	312.0 ÷ 327.4
NIST – NPL	Transatlantic	7 118 km	312.0 ÷ 326.2

A. *Double Differences Results*

Fig. 3 gives the double difference comparison between PPP and TWSTFT for two different baselines, NPL-OP and OP-NIST. In these double differences, the reference clocks are completely removed and residual biases are intended to assess the level of agreement between these two completely independent synchronization techniques.

Residual biases in the double differences fall within ±1.0 ns with less than 500 ps standard deviation. Note the 2-week boundary discontinuity that takes place in the second half of the interval. However, it is worth mentioning that in this experiment the comparison between PPP and TWSTFT seems to be highly driven by the short-term noise affecting TWSTFT, especially for Transatlantic baselines involving NIST laboratory, as confirmed by the frequency stability results reported in the following section.

B. *Frequency Stability*

Computing the stability of the comparison data between PPP and TWSTFT for the selected baselines, the results shown in Fig. 4 in terms of overlapping Allan deviation are obtained.

The measurement noise introduced by PPP is a factor of 1.5 lower than TWSTFT (at least for short baseline) for observation periods varying from 2 hours up to 1 day and even longer. After that, the two methods come together approaching the nominal behavior of H-masers of the two stations, i.e. a flicker floor of $4 \cdot 10^{-15}$ up to about 3 days.

On the other hand, looking at the double differences between TWSTFT and PPP, it can be noticed that, since measurement noise is dominant, the noise exhibited represents contribution of the noisier of the two measurement systems. For longer averaging times (1 day and longer), the double differences go down with a τ^{-1} slope resulting in decreasing measurement uncertainty when longer observation times are considered.

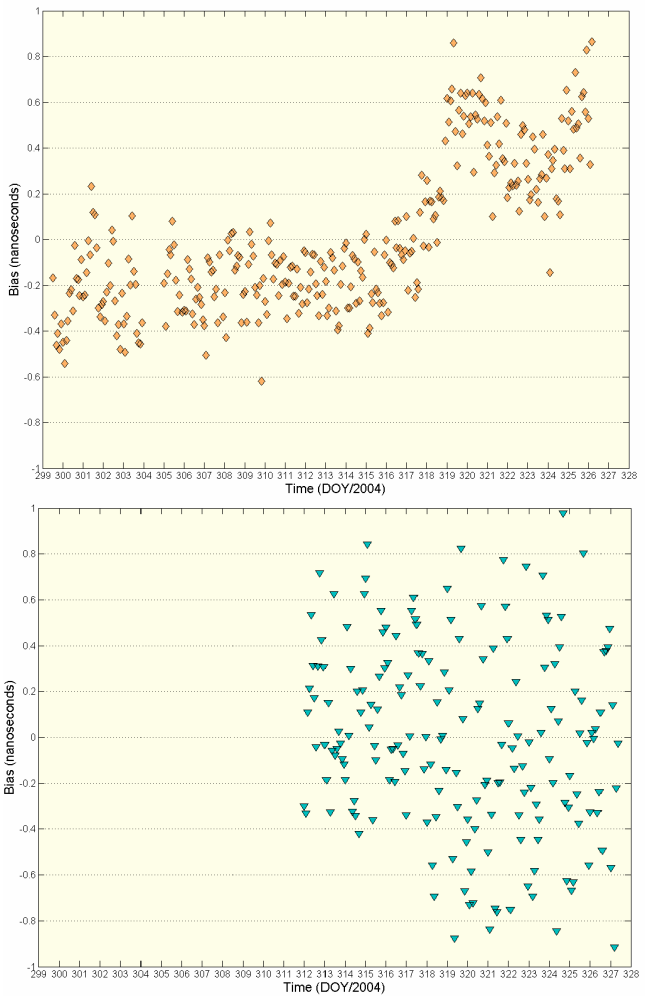

Figure 3. Double differences between PPP estimates and TWSTFT data for the NPL to OP European link (27 days, upper plot) and for the OP to NIST Transatlantic link (16 days, lower plot).

Moreover, a significant improvement using PPP is clearly noticed for the very long OP–NIST baseline, showing that PPP performance seems to be independent of baseline attributes, e.g. the distance between stations. Of course, the figure exhibited by TWSTFT link with NIST during this experiment doesn't represent its typical quality, and it could be due to poor performance of the dedicated transponder on the Intelsat geostationary satellite at that time.

C. *Frequency Transfer*

Aiming to take a preliminary look at the frequency comparison potential of PPP, the relative frequency difference between couples of H-maser for the three selected baselines (Table VIII) have been computed. The frequency values have been simply calculated as

$$y(t) = [\delta_{ck}(t) - \delta_{ck}(t - T)] / T \qquad (1)$$

where $\delta_{ck}(t)$ is the time difference at epoch t between the PPP clock offset estimates of the two stations involved in the baseline, and T is the measurement interval (i.e., 300 seconds). These values have been then compared with those coming out from TWSTFT data, for the period of intensified schedule operated by some timing laboratories during the Cs fountains comparison campaign [11]. Results are given in Fig. 5, where a significant reduction of noise achieved by PPP is clearly noticed, especially for Transatlantic baselines.

Comparing the mean frequencies computed in Table IX, the TWSTFT and PPP methods match very well, at the level of $1.2 \cdot 10^{-15}$. Moreover, an expected zero closure is achieved by PPP, because PPP estimates are site-based. In contrast, TWSTFT results show a $-0.6 \cdot 10^{-15}$ departure from zero, mainly due to the fact that TWSTFT measurements are not simultaneously performed and the clock rates have to be then considered.

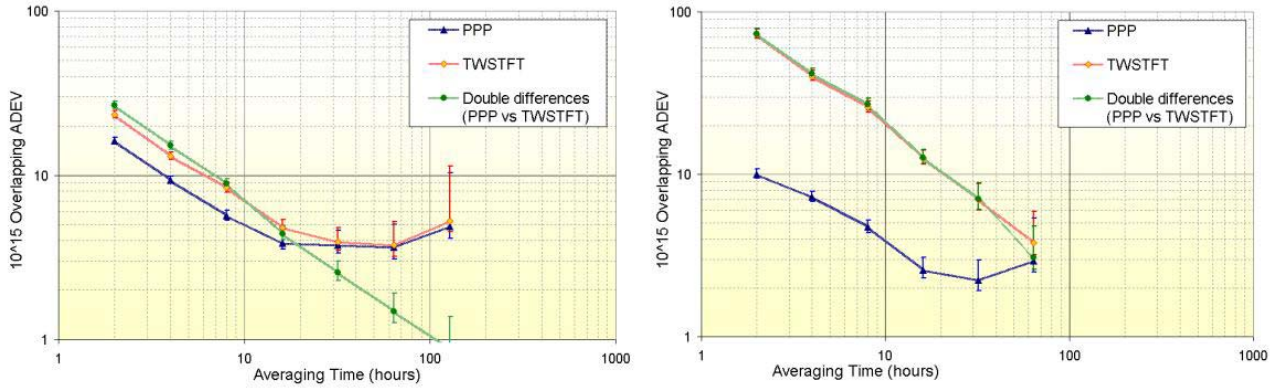

Figure 4. Frequency stability comparison (in term of Allan deviation) between PPP (blue triangles) and TWSTFT (red diamonds) for the NPL to OP European link (left plot) and for the OP to NIST Transatlantic link (lower plot). Residuals between the two techniques are also depicted (green circles).

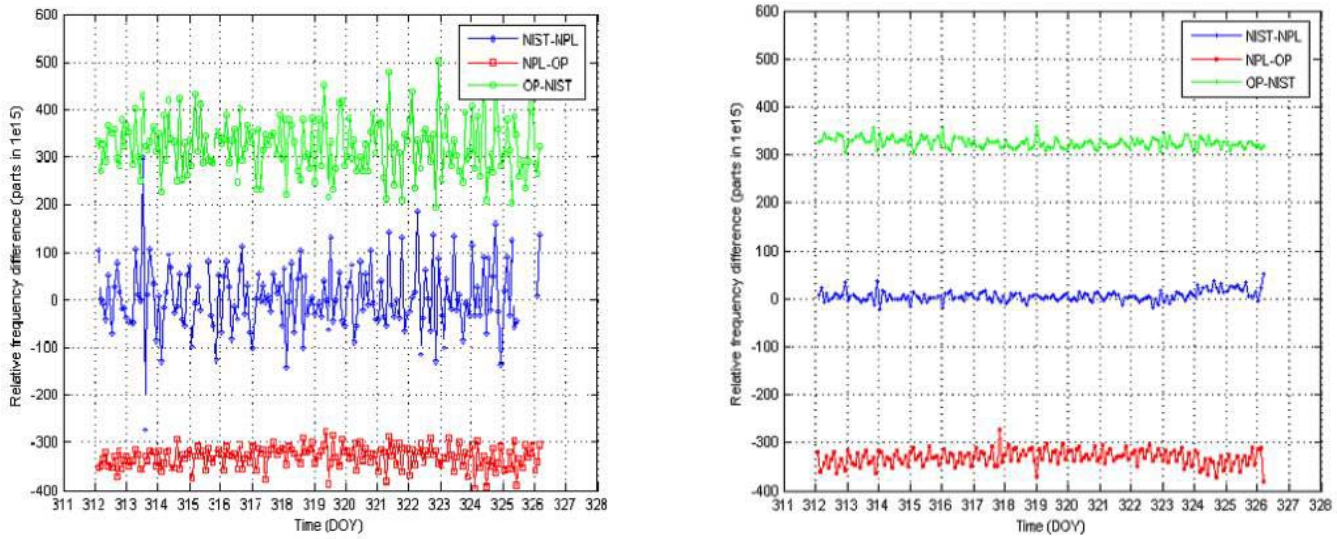

Figure 5. Relative frequency difference between couples of H-masers located in NIST, OP and NPL laboratories (see legend for details) using TWSTFT (left plot) and PPP (right plot) estimates, for the period from DOY 312/2004 to 326/2004 (inclusive, 15 days).

TABLE IX. MEAN RELATIVE FREQUENCY DIFFERENCE (IN PARTS OF 10^{15}) USING TWSTFT AND PPP ESTIMATES.

Method	NIST-NPL	NPL-OP	OP-NIST	Closure
TWSTFT	4.7	-330.1	324.8	-0.6
PPP	5.9	-330.9	325.0	0.0

VII. CONCLUSIONS

Results from the experimental activity reported in this paper make PPP a promising additional synchronization technique offering high-level performance comparable with "state-of-art" methods, such as the TWSTFT.

Without arrangement of any network solution, PPP autonomously provides recovery of IGS combined clock solution at sub-ns level (130 ps RMS for all selected stations). Besides, running continuously for periods of up to 2 weeks, the current NRCan PPP software is able to reduce the artificial solution-boundary discontinuities, allowing then specific time-limited campaign (e.g., PFS comparison).

In addition, comparison with a completely independent synchronization technique, i.e. TWSTFT, results in a very good agreement showing double differences less than 1 ns after removing a mean offset to account for any calibration between different equipment. Besides, it has been observed that the measurement noise introduced by PPP seems a factor of 1.5 lower than TWSTFT (for observation times up to 1 day) over European baseline and potentially more on Transatlantic baselines, PPP performance being independent of the geographical separation of the time link.

Also, possible re-use of existing geodetic GPS receivers and low-cost investment (i.e., less than 10 kEuro) in the event that new equipment has to be procured, are valuable advantages of PPP for timing laboratories. Moreover, it is worth mentioning that no bureaucratic procedures are required with PPP, unlike TWSTFT where authorization to transmit in Ku-band is a mandatory requirement of the transponder provider.

However, further assessment of the PPP geodetic time transfer method is recommended, and following improvements to NRCan PPP software should be addressed:

- improve the robustness of data editing, as well as the detection and discrimination between carrier phase reset and clock jump, aiming to improve the continuity of the PPP clock estimates time series;
- generalize the internal clock model to accept a wider range of external frequency standards, e.g. free-running H-masers;
- investigate the anomalous "bump" observed in the Allan deviation (section V);
- assess the significance of the increased size of solution-boundary clock discontinuities when processing on longer continuous intervals.

ACKNOWLEDGMENT

The authors wish to thank all the people in timing laboratories involved in this experiment for granting the use of their GPS and TWSTFT data. Their contribution is highly appreciated.

The authors wish to acknowledge the many individuals and institutions forming the IGS for the high quality GNSS products and data without which the PPP timing application reported herein would not be possible.

Special thanks are due to colleagues at NRCan for continued improvement of the PPP software, namely Pierre Tétreault, Pierre Héroux and especially Jan Kouba, and to Giancarlo Cerretto and other students with the IEN Time and Frequency Laboratory for the helpful support in data retrieving and processing.

REFERENCES

[1] J. Ray and K. Senior, "Geodetic techniques for time and frequency comparisons using GPS phase and code measurements," Metrologia, vol. 42, 2005, pp. 215-232.

[2] R. Dach, U. Hugentobler, T. Schildknecht, L.-G. Bernier, and G. Dudle, "Precise Continuous Time and Frequency Transfer Using GPS Carrier Phase," in these Proceedings.

[3] J. Ray and K. Senior, "IGS/BIPM pilot project: GPS carrier phase for time/frequency transfer and timescale formation," Metrologia, vol. 40, 2003, pp. S270-S288.

[4] K. Senior, P. Koppang and J. Ray, "Developing an IGS time scale," IEEE Trans. Ultrasonic Ferrolectric Frequency Control (UFFC), vol. 50, 2003, pp. 585-593.

[5] J. Kouba and T. Springer, "New IGS station and satellite clock combination," GPS Solutions, vol. 4, 2001, pp. 31-36.

[6] J. Kouba and P. Héroux, "Precise Point Positioning Using IGS Orbit and Clock Products", GPS Solutions, vol. 5 n. 2, 2001, pp. 12-28.

[7] R. Costa, D. Orgiazzi, V. Pettiti, I. Sesia and P. Tavella, "Performance Comparison and Stability Characterization of Timing and Geodetic GPS Receivers at IEN," in Proceedings of the 18th European Time and Frequency Forum (EFTF), Guildford, UK, 5-7 April, 2004.

[8] C. Bruyninx, P. Defraigne, J. Ray, F. Roosbeck and K. Senior, "Comparison of Geodetic Clock Analysis Strategies," 36th Annual Precise Time and Time Interval (PTTI) Systems and Applications Meeting, Washington D.C., USA, 7-9 December, 2004, unpublished.

[9] P. Defraigne, G. Petit and C. Bruyninx, "Use of geodetic receivers for TAI," in Proceedings of 33rd Annual Precise Time and Time Interval (PTTI) Systems and Applications Meeting, Washington D.C., USA, 2001, pp. 341-348.

[10] ftp://igscb.jpl.nasa.gov/igscb/data/format/rinex210.txt.

[11] A. Bauch, J. Achkar, R. Dach, R. Hlavac, L. Lorini, T. Parker, G. Petit and P. Uhrich, "Time and Frequency Comparisons Between Four European Timing Institutes and NIST Using Multiple Techniques," in Proceedings of the 19th European Time and Frequency Forum (EFTF), Besançon, France, 21-24 March, 2005, in press.

[12] R. Dach, T. Schildknecht, U. Hugentobler, L.-G. Bernier and G. Dudle, "Continuous geodetic time transfer analysis methods," in Proceedings of the 2004 IEEE International Frequency Control Symposium and Exposition, 23-27 August, 2004, pp. 350-350.

[13] BIPM, Consultative Committee for Time and Frequency (CCTF), http://www1.bipm.org/en/committees/cc/cctf/working_groups.html.

[14] Recommendation ITU-R TF.1153-1, "The operational use of two-way satellite time and frequency transfer employing PN time codes," ITU, Radiocommunication Study Group, Geneva, last update 2003.

[15] IGS Mail #5078, http://igscb.jpl.nasa.gov/mail/.